Correlating Cellular Morphology, Physiology, and Gene Expression Using Patch-seq

Cathryn R. Cadwell, PhD, and Andreas S. Tolias, PhD

Department of Neuroscience
Baylor College of Medicine
Houston, Texas

SOCIETY *for* NEUROSCIENCE

Introduction

More than a century ago, Ramon y Cajal and others speculated that even the most complex functions of the human brain—perception, memory, and decision-making—might eventually be understood at the level of neuronal cell types and their connections (Cajal et al., 2002). Since that time, it has become increasingly clear that different brain regions contain distinct molecularly specified neuronal cell types with characteristic morphological and electrophysiological properties. Furthermore, these different kinds of neurons are arranged in stereotypical circuits that are essential to the functions that each brain area performs. True understanding of the workings of the normal and pathological brain will require identification of all the constituent cell types, mapping their interconnections, and determining their function *in vivo*.

Approaches to Cell-Type Classification

For decades, the gold standard for classification of neuronal cell types has been their complex and diverse morphology (Cajal et al., 2002; Burkhalter, 2008; Petilla Interneuron Nomenclature Group et al., 2008). In particular, axonal geometry and projection patterns have been the most informative morphological features for predicting how a neuron is integrated into the local circuit (Burkhalter, 2008). To better understand the extensive diversity of cell types in the neocortex and how they are connected into functional circuits, we recently performed a census of morphologically defined neuronal types (primarily GABAergic interneurons) in adult mouse visual cortex layers 1, 2/3, and 5 (L1, L2/3, and L5) using octuple simultaneous, whole-cell patch-clamp recordings, and an improved avidin–biotin–peroxidase staining technique that allowed detailed recovery of axonal and dendritic arbor morphology (Fig. 1) (Jiang et al., 2015). We identified 15 major types of interneurons, each of which has stereotypical electrophysiological properties and morphological features and can be differentiated from all others by cell-type-specific axonal geometry and axonal projection patterns. Notably, each type of neuron has its own unique input–output connectivity profile, connecting with other constituent neuronal types with varying degrees of specificity in postsynaptic targets, laminar location, and synaptic characteristics. Despite specific connection patterns for each cell type, we found that a small number of simple
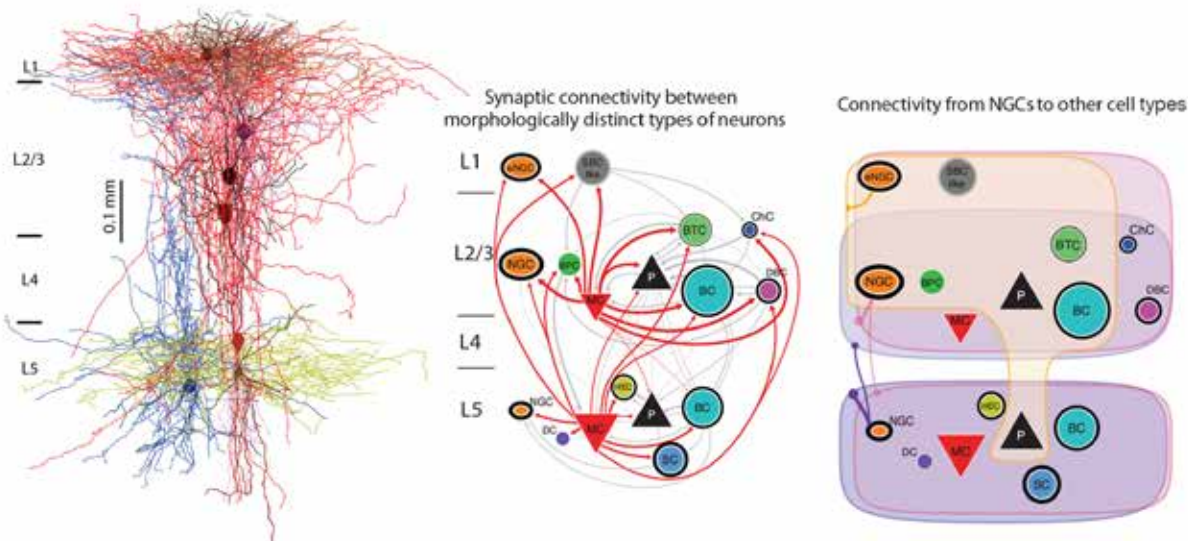

Figure 1. Connectivity among morphologically defined cell types in adult neocortex. Left panel, simultaneous octuple whole-cell recording to study connectivity followed by morphological reconstruction. Scale bar, 0.1 mm. Middle panel, synaptic connectivity among morphologically distinct types of neurons, including pyramidal neurons. Right panel, connectivity from NGCs to other cell types. This connectivity is believed to be nonsynaptic and mediated by volume transmission. B, basket cell; BP, bipolar cell; BT, bitufted cell; Ch, chandelier cell; D, deep projecting cell; DB, double bouquet cell; E, horizontally elongated cell; M, Martinotti cell; NG, neurogliaform cell; P, pyramidal neuron; S, shrub cell. Adapted from Jiang X et al., 2015, Principles of connectivity among morphologically defined cell types in adult neocortex, Science 350:aac9462, their Figs. 3*A*, 6*A*, and 6*B*, with permission from AAAS.

connectivity motifs are repeated across layers and cell types, defining a canonical cortical microcircuit.

Recent advances in molecular biology, particularly high-throughput single-cell RNA-sequencing (RNA-seq) (Tang et al., 2009; Sandberg, 2014), have begun to reveal the rich genetic programs that give rise to cellular diversity (Fishell and Heintz, 2013). These advances have enabled *de novo* identification of cell types in many tissues, including neuronal subtypes in the retina, neocortex, and hippocampus (Macosko et al., 2015; Zeisel et al., 2015; Tasic et al., 2016). Unfortunately, it has been difficult to reconcile these molecular classification schemes with the classical morphologically defined cell types (Burkhalter, 2008; Petilla Interneuron Nomenclature Group et al., 2008; DeFelipe et al., 2013). Currently available transgenic lines for targeting molecular subclasses of neurons paint a picture of the cortex in broad strokes, with insufficient resolution to distinguish many of the known morphologically defined cell types. For instance, in our study of interneuron subtypes, we recorded from three widely used transgenic lines (targeting parvalbumin [PV]–expressing, somatostatin [SST]–expressing, and vasoactive intestinal peptide [VIP]–expressing interneurons). We found that each molecular class included a number of distinct morphological subtypes, some of which were identified in more than one molecular class, and some of which were not represented in any of the lines (Jiang et al., 2015). Novel molecular markers and techniques to correlate gene expression and morphology at the level of single cells are therefore needed to arrive at a comprehensive cell-type classification scheme that incorporates molecular, morphological, and physiological criteria.

Development of the Patch-seq Protocol

We developed a protocol called Patch-seq that combines whole-cell patch-clamp recordings with high-quality RNA-seq of single neurons, and used L1 of the mouse neocortex as a simple proof of principle to demonstrate the feasibility of this approach to cell-type classification (Cadwell et al., 2016). L1 is known to contain only two main morphological classes of neurons, both of which are inhibitory interneurons, with their own distinct firing patterns and connectivity profiles: elongated neurogliaform cells (eNGCs) and single bouquet cells (SBCs) (Jiang et al., 2013). Using standard electrophysiology techniques in cortical slices, we first generated

a dataset of 72 L1 interneurons, for which we recorded their firing pattern in response to sustained depolarizing current and also reconstructed their detailed morphology using avidin–biotin–peroxidase staining (Figs. 2*a, b*). Using this as training data, we built an automatic cell-type classifier based on electrophysiological properties that could predict morphological cell class with ~98% accuracy (Figs. 2*d, e*). In a separate set of experiments, we patched an additional set of 67 L1 interneurons in acute cortical slices using the Patch-seq protocol. This protocol makes use of an optimized mechanical recording approach (tip size, volume inside pipette, etc.) as well as a modified intracellular recording solution to extract and preserve as much full-length mRNA from each cell as possible (see Cadwell et al., 2016, for a detailed protocol). For downstream RNA-seq analysis, we recorded their firing patterns (Fig. 2*c*) and extracted their cell contents until the cell had visibly shrunken (Fig. 2*g*). Each neuron from this RNA-seq dataset was assigned to a neuronal class of either eNGC or SBC by blinded expert examination of the firing pattern and using the automated classifier just described. Both classifications were performed independently and led to very similar cell-type labels ($r = 0.91$) (Fig. 2*f*). In addition, we recorded from 32 L1 interneurons *in vivo* in anesthetized animals and extracted their cell contents for RNA-seq. Large fluctuations in the resting membrane potential, likely resulting from ongoing activity in the local circuit and/or fluctuations in cortical state (Reimer et al., 2014), made it difficult to classify neurons recorded *in vivo* based on their electrophysiological properties. Thus, these cells did not receive a cell-type label. Although we aimed to target L1 interneurons, we occasionally patched an excitatory neuron ($n = 1$ *ex vivo*; $n = 7$ *in vivo*) or astrocyte ($n = 1$ *in vivo*) near the L1/L2 border. Rather than discarding these samples, we proceeded with RNA-seq in the same manner as for the L1 interneurons and used them as additional controls to validate cell-type-specific markers (see below). In addition, each experiment included at least one negative control, in which a recording pipette was inserted into the tissue but no cell was patched. The negative controls were processed in the same manner as the rest of the samples to assess the amount of background contamination during sample collection and amplification.

After harvesting the cell contents, single-cell mRNA was converted to cDNA and used to generate sequencing libraries following a protocol similar to Smart-seq2 (Picelli et al., 2013; Cadwell et al., 2016). Libraries with low cDNA yield (<200
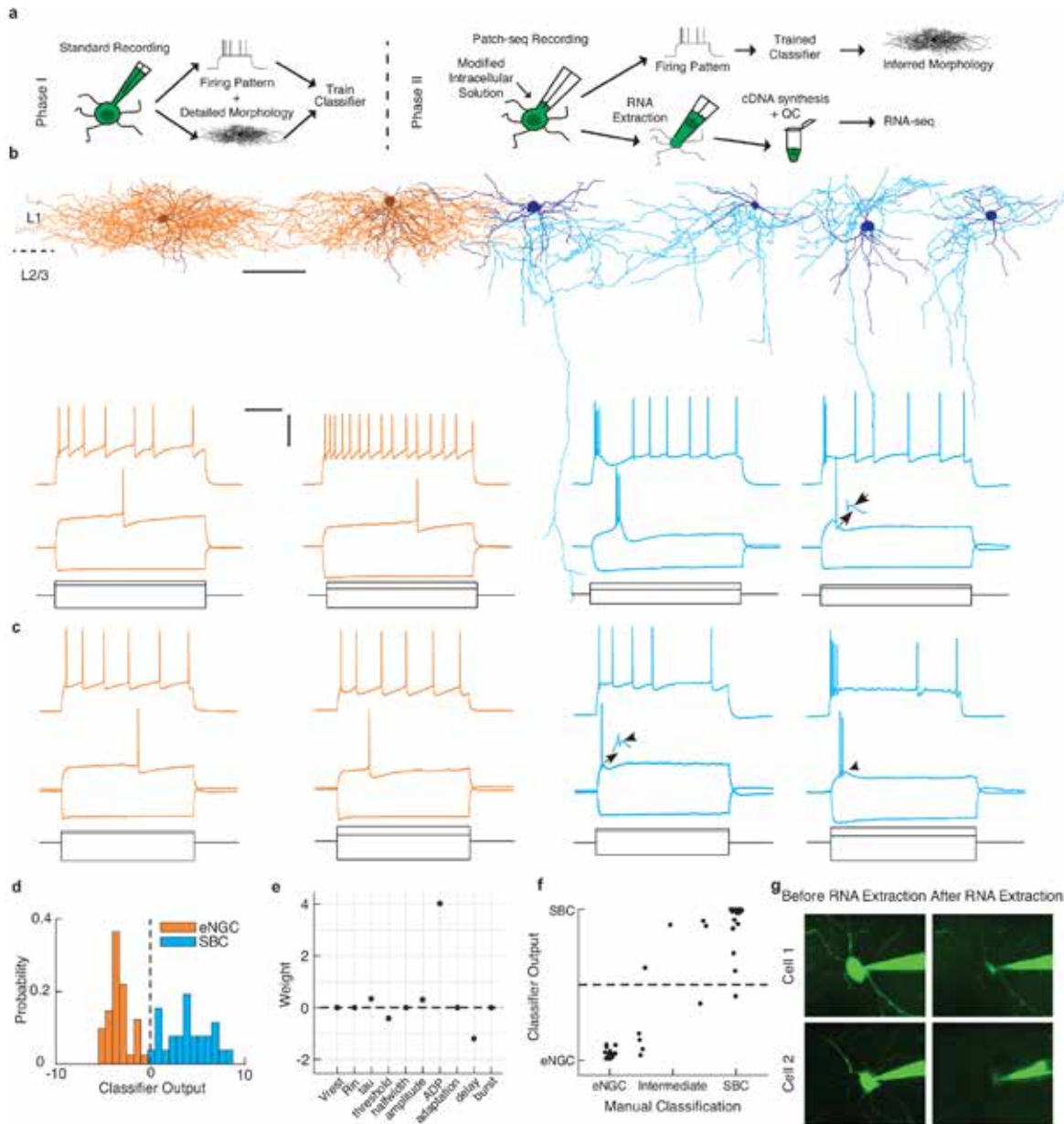
Figure 2. Two morphologically and electrophysiologically distinct neuronal classes in neocortical L1. *a*, Schematic of experimental approach. QC, quality control. *b*, Representative examples of the morphology (top) and firing pattern (bottom) of the two main types of neurons found in L1: eNGCs (orange) and SBCs (cyan). For morphological reconstructions, the darker outline represents the somatodendritic region, and the lighter color is the axonal arbor. Scale bar, 100 μm. For firing patterns, gray lines represent current steps used to elicit the firing patterns shown above. Scale bars, 300 ms (horizontal bar), 40 mV and 500 pA (vertical bar). Arrows denote prominent after-depolarization in SBCs. *c*, Neurons recorded using Patch-seq protocol display similar firing responses as seen using standard electrophysiological techniques, as shown in *b*. *d*, Output of automated cell-type classifier robustly predicts morphological class based on electrophysiological features. *e*, Weights of features used in the automated cell-type classifier. *f*, Results of the automated classifier highly correlate with an independent, blinded expert classification of the electrophysiological properties as "eNGC-like" or "SBC-like"; $r = 0.91$. *g*, Example cells before and after RNA extraction. Reprinted with permission from Cadwell CR et al., 2016, Electrophysiological, transcriptomic and morphologic profiling of single neurons using Patch-seq, Nat Biotech 34:199–203, Fig. 1. Copyright 2016, Nature Publishing Group.

pg/µl) or poor quality suggesting cDNA degradation (<1500 bp mean size) were excluded from further analysis (50/108 cells and 32/32 negative controls). A higher fraction of *in vivo* samples was excluded (31/40) compared with *ex vivo* samples (19/68), likely because of a combination of lower amounts of cDNA obtained as well as increased contamination during *in vivo* sample acquisition (i.e., the pipette must penetrate the dura and traverse more tissue in order to reach the target cell). We sequenced the 58 single-cell libraries that met our inclusion criteria; they corresponded to 48 L1 interneurons patched in slices, 5 L1 interneurons patched *in vivo*, 1 pyramidal neuron patched in slices, 3 pyramidal neurons patched *in vivo*, and 1 astrocyte patched *in vivo*. Analyses of the sequenced libraries revealed that, on average, 65% of reads mapped uniquely to the mouse genome, and 60% of those mapped within exons. As expected, the pyramidal neuron and astrocyte samples showed clear differences in gene expression compared with the L1 interneurons (Fig. 3*a*) (Cadwell et al., 2016), consistent with known cell-type-specific markers (Bignami et al., 1972; Marshak, 1990; Chan et al., 2001; Fremeau et al., 2001). We subsequently focused our analyses on the L1 interneurons, which expressed interneuron markers including *Gad1*, *Reln*, and *Cplx3* (Alcantara et al., 1998; Stuhmer et al., 2002). We detected ~7000 genes per interneuron (Fig. 3*b*), with an average Spearman correlation of 0.59 and 0.56 between *ex vivo* and *in vivo* cells, respectively (Fig. 3*c*). This result was on par with those of high-quality cDNA libraries used for molecular cell-type classification in other tissue types (Jaitin et al., 2014; Treutlein et al., 2014) and had a higher detection of genes per cell than a recent study using dissociated neurons (Zeisel et al., 2015).

Correlation of Morphology, Physiology, and Gene Expression Using Patch-seq

In order to explore the interneuron transcriptomes and to resolve the molecular cell classes in an unbiased manner, we performed unsupervised clustering and dimensionality reduction analysis using the 3000 most variable genes. Affinity propagation was used to cluster cells in this high-dimensional gene space (without prespecifying the number of clusters), and we reduced the dimensionality of the data to visualize the resulting clusters using *t*-distributed stochastic neighbor embedding (*t*-SNE). We identified two molecular interneuron clusters (Fig. 3*d*) (Cadwell et al., 2016) with high correspondence to the eNGC and SBC classification (41/47 cells, 87%) (Figs. 3*d, e*). Random subsampling of the data demonstrated that the two cell classes could be robustly distinguished

using as few as 31 samples. In addition, we asked whether we could predict cell class based on single-cell gene expression using a regularized generalized linear model (GLM). The classifier performed at ~86% accuracy for predicting cell type (Fig. 3*f*). Together, these results demonstrate a strong agreement between cell-type assignments based on morphological, electrophysiological, and transcriptional profiles.

Next we asked whether specific physiological properties could also be predicted using single-neuron gene expression data. We trained a sparse, regularized GLM for each of seven quantitative electrophysiological measurements using the single-cell transcriptome data (selecting the most variable 50–250 genes across cells) as input. Three of these measurements (after-hyperpolarization amplitude [AHP], after-depolarization amplitude [ADP], and action potential [AP] amplitude) could be predicted based on differential gene expression, as shown by the correlation between cross-validated predictions and the ground truth for individual neurons (Figs. 3*g–i*). The remaining variables (membrane time constant, adaptation index, AP width, and resting membrane potential) could not be modeled using gene expression data, suggesting either that variability along these features may reflect factors other than differential gene expression or that a larger dataset is needed to infer these properties from single-cell gene expression.

Transcriptome analyses of cells collected *in vivo* assigned many of them to a specific cell class (Fig. 3*e*). They also suggested a shift in gene expression compared with cells collected *ex vivo* (Fig. 3*e*, second *t*-SNE component [tSNE2]) that may reflect an increased stress response in the acute slice preparation (e.g., increased *Fos* expression *ex vivo* compared with *in vivo*). Notably, these results demonstrate that high-quality, whole-transcriptome data can be obtained even from single neurons in intact animals, and that the gene expression profile within a cell class is mostly preserved across *in vivo* and *ex vivo* preparations. Extension of cell-type classification to include dynamic functional properties, such as receptive fields and tuning properties (which can be measured only *in vivo*) may ultimately lead to better understanding of cell types in terms of their role in information processing in the cortex.

Identification of Novel Cell-Type Markers Using Patch-seq

Cell-type-specific transcriptome data can be used to generate improved driver lines for cell-type targeting. As noted earlier, current genetic cell-type-specific
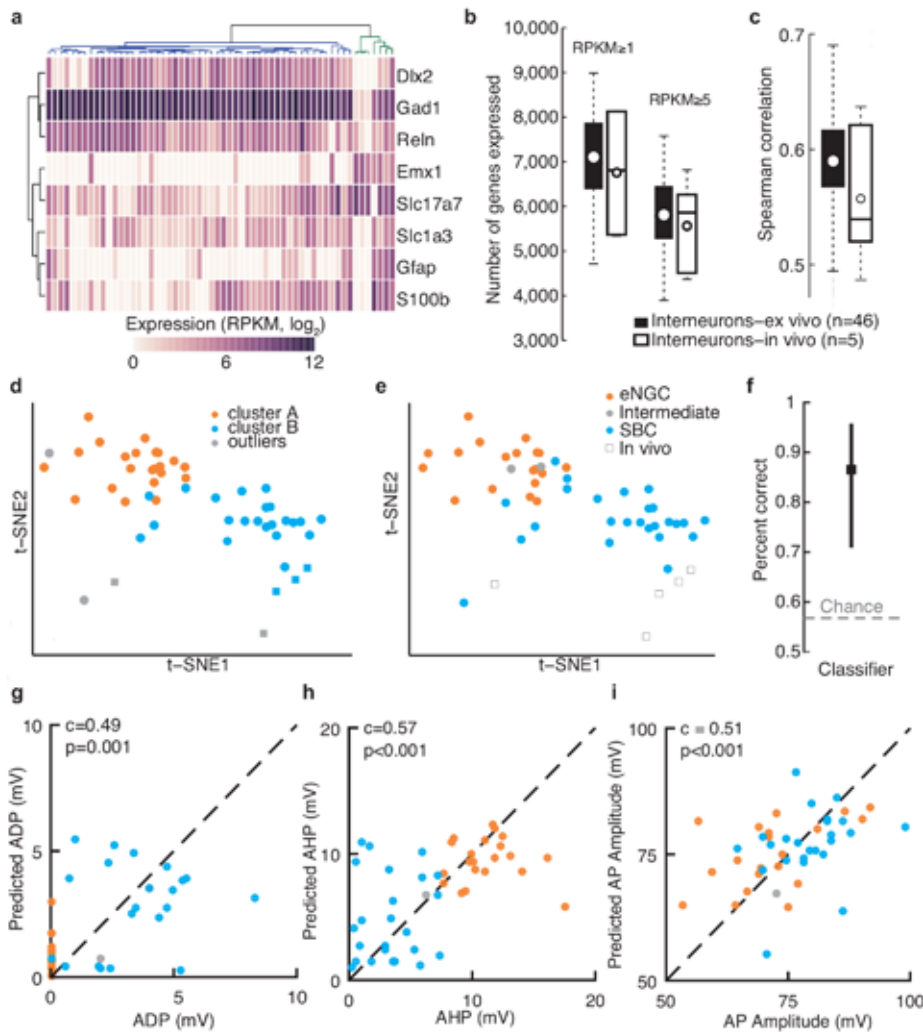
Figure 3. Single-neuron transcriptome profiles predict cell type and electrophysiological properties. *a*, Clustering analysis separates interneurons (blue dendrogram subtree) from other neuronal classes (green dendrogram subtree, includes four pyramidal neurons and one astrocyte) based on marker gene expression. Two L1 interneurons clustered with non-interneuron cell types, indicating possible contamination of these samples, and so these two cells were excluded from our analysis of interneuron subtypes. *b*, Number of genes detected per neuron using two different expression thresholds, shown for both *ex vivo* and *in vivo* collection methods. *c*, Pairwise Spearman correlation across all detected genes for *ex vivo* and *in vivo* patched interneurons. *d*, Two-dimensional *t*-SNE representation of gene expression for all L1 interneurons. Cells are colored according to affinity propagation–based clustering in gene space spanned by the 3000 most variable genes before dimensionality reduction. *e*, The same two-dimensional map as in *d*, but with cells color-coded according to expert classification of cell type based on electrophysiological properties. Performance of GLMs using single-neuron gene expression to predict cell type (*f*), ADP (*g*), AHP (*h*), or AP amplitude (*i*). RPKM, reads per kilobase of transcript per million reads. Reprinted with permission from Cadwell CR et al., 2016, Electrophysiological, transcriptomic and morphologic profiling of single neurons using Patch-seq, Nat Biotech 34:199–203, Fig. 2. Copyright 2016, Nature Publishing Group.

markers often lack sufficient specificity to capture the known diversity of morphological cell classes (Burkhalter, 2008; Petilla Interneuron Nomenclature Group et al., 2008; Jiang et al., 2015). In the case of L1 interneurons, previous studies have suggested that late-spiking eNGCs express Reelin, whereas burst-spiking SBCs express vasoactive intestinal peptide (VIP) (Miyoshi et al., 2010). However, other studies have shown that Reelin is found in similar proportions of both cell types, and only ~20% of burst-spiking cells express VIP (Ma et al., 2014). We found that neither of these markers was very useful for distinguishing eNGCs from SBCs at the mRNA level (Fig. 4a). This finding calls into question whether single-neuron reverse transcriptase (RT)–PCR and protein-level studies are well suited for predicting

which mRNA transcripts are differentially expressed between cell types. Using single-cell differential expression (SCDE) analysis (Kharchenko et al., 2014), we identified several genes that are strongly differentially expressed between the two cell types (Fig. 4b). These genes have the potential to serve as more robust cell-type markers and facilitate future studies on the functional roles of these cell types in the cortical microcircuit.

Patch-seq Provides Insight Into Mechanisms of Synaptic Specificity and Disease Pathophysiology

In the past several decades, we have witnessed a revolution in human genetics that has revealed hundreds of gene mutations that correlate with neuropsychiatric disorders such as autism spectrum
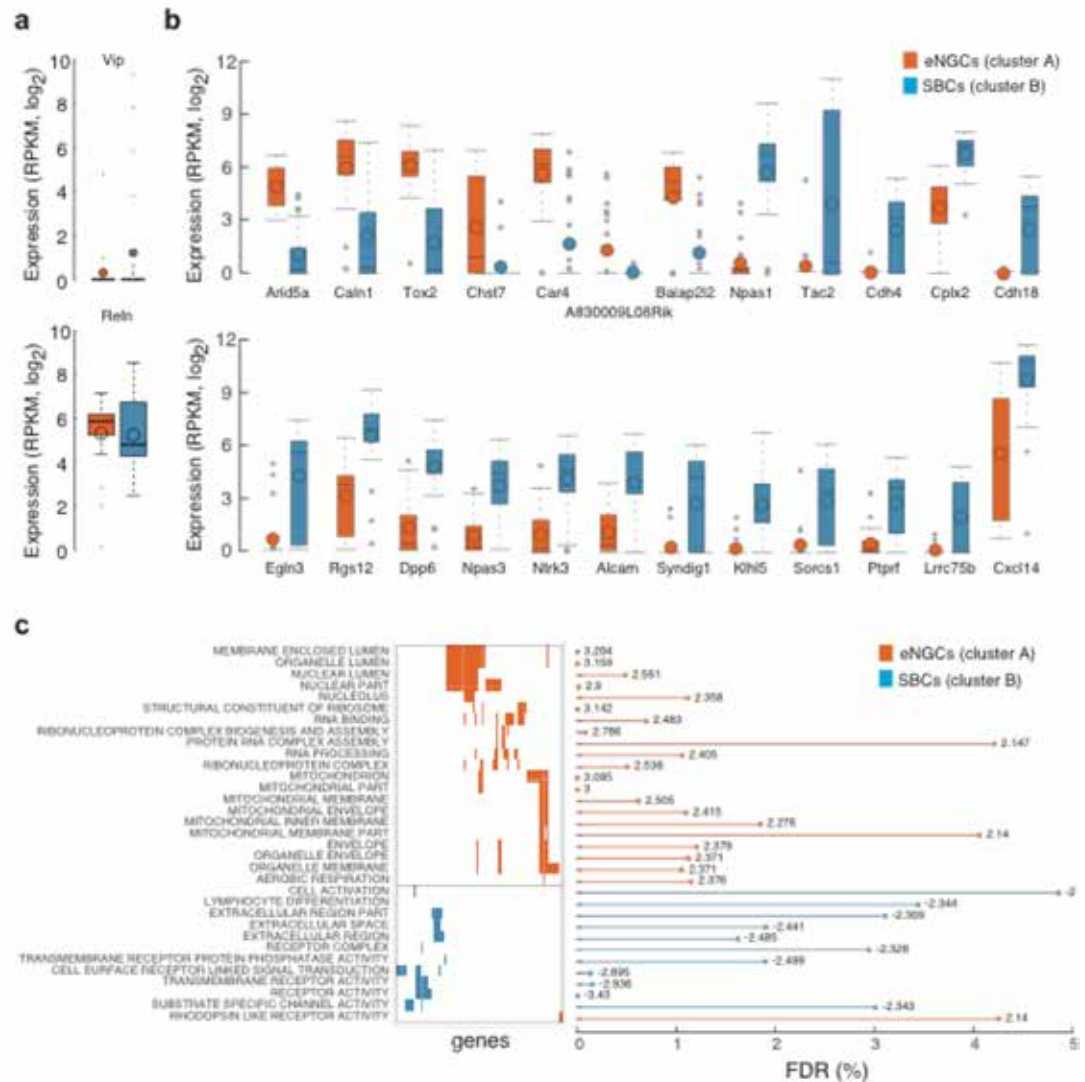

Figure 4. Differential gene expression analysis reveals novel markers for L1 interneuron classes. *a*, Box plots summarize the cell-type expression level of previously proposed marker genes (*Vip* and *Reelin*). *b*, Box plots with expression levels across cell types for novel differentially expressed genes identified between the two affinity propagation clusters. *c*, Significant gene ontology categories from GSEAs on ranked genes from SCDE analysis of SBCs and eNGCs. The gene matrix illustrates gene overlap among categories; the bar plot shows the false discovery rates (FDR), and the numbers indicate normalized enrichment scores per category from GSEA. RPKM, reads per kilobase of transcript per million reads. Reprinted with permission from Cadwell CR et al., 2016, Electrophysiological, transcriptomic and morphologic profiling of single neurons using Patch-seq, Nat Biotech 34:199–203, Fig. 3. Copyright 2016, Nature Publishing Group.

disorders, schizophrenia, and depression. Many of these disease-related genes have been linked to synapse formation and function (Spooren et al., 2012; Delorme et al., 2013). However, the expression of disease-associated genes has not been systematically mapped to specific cell types or circuits. Knowing which cell type(s) a disease-associated gene is expressed in is crucial to understanding the disease mechanism and developing novel therapeutic strategies (Siegert et al., 2012). Moreover, having reference transcriptomes for different neuronal cell types will facilitate cell-type engineering through the reprogramming of pluripotent stem cells into specific types of neurons and could lead to more principled treatments for neurological disorders.

In our study of L1 interneurons, gene set enrichment analysis (GSEA) revealed that genes involved in cell–cell signaling (transmembrane and extracellular proteins, receptors, ion channels, and intracellular signaling molecules) were particularly upregulated in SBCs, whereas genes involved in RNA processing and mitochondrial function were upregulated in eNGCs (Fig. 4c). These findings are consistent with previous reports that eNGCs communicate nonspecifically with all cell types using volume transmission, whereas SBCs form highly selective synapses onto particular neuronal types (Olah et al., 2009; Jiang et al., 2013, 2015). In particular, our results predict that increased expression of cell adhesion molecules (including CDH18 [cadherin 18], CDH4, and ALCAM [activated leukocyte cell adhesion molecule]) and synaptic regulatory proteins (such as SYNDIG1 [synapse differentiation inducing 1]) may play an important role in shaping the synaptic specificity of SBCs (Jiang et al., 2013, 2015). Taken together, these results demonstrate that whole-transcriptome profiling of patched neurons is a useful approach to identify novel, unpredicted mechanisms of synaptic specificity.

A number of the differentially expressed genes we identified are also associated with human disease. For example, the genes encoding the transcription factors NPAS1 (neuronal PAS domain protein 1) and NPAS3 are highly expressed in SBCs but not in eNGCs (Fig. 4b). Notably, these proteins have been implicated in autism spectrum disorders (ASD) and schizophrenia and were previously shown to regulate the generation of specific neocortical interneurons (Macintyre et al., 2010; Stanco et al., 2014). SBCs also preferentially express *Dpp6* (dipeptidylpeptidase 6) and *Cplx2* (complexin 2) (Fig. 4b). DPP6 is an auxiliary subunit of the Kv4 family of voltage-gated K^+ channels implicated in ASD that regulates channel function and dendrite morphogenesis (Lin et al., 2013), whereas CPLX2 is a presynaptic protein linked to schizophrenia that controls neurotransmitter release and presynaptic differentiation (Brose, 2008). Our observation that four disease genes implicated in neuropsychiatric illness are significantly upregulated in SBCs, combined with previous studies suggesting that SBCs may play an important role in the detection of salient sensory information and the mediation of top-down influences (Jiang et al., 2013), raises the question of whether SBC dysfunction may contribute to the pathophysiology of autism and schizophrenia. The ability to map disease-associated genes onto specific neuronal cell types will lay the foundation for a more principled, circuit-level understanding of neuropsychiatric disorders.

Conclusions and Future Directions

Generating a complete census of neocortical cell types that integrates morphological, electrophysiological, and gene expression data into a cohesive classification scheme presents a tremendous challenge for the field of neuroscience. We have developed a technique to bridge these three distinct modalities, bringing them into a common framework by combining whole-cell patch-clamp recordings and high-quality RNA-sequencing of individual neurons. Using Patch-seq, we demonstrated that cellular morphology, physiology, and gene expression can be integrated at the single-cell level to generate a comprehensive profile of neuronal cell types, using neocortical L1 interneurons as a proof of principle. In addition, we identified several molecular markers that can be used to target these cell types for further study, generate new hypotheses regarding the molecular mechanisms of their synaptic specificity, and link specific cell types to neuropsychiatric illness. Notably, this approach can be used broadly to characterize neuronal cell types in any brain region, in different mouse models of disease, and even in nongenetically tractable organisms such as primates. We hope that the ability to perform unbiased, whole-genome transcriptome analysis and to physiologically characterize individual neurons will help to resolve long-standing questions in the field of neuroscience and initiate entirely new directions of investigation.

Acknowledgments

neurons using Patch-seq. Nat Biotech 34:199–203. Copyright 2016, reprinted with permission from Nature Publishing Group.

References

Alcantara S, Ruiz M, D'Arcangelo G, Ezan F, de Lecea L, Curran T, Sotelo C, Soriano E (1998) Regional and cellular patterns of *reelin* mRNA expression in the forebrain of the developing and adult mouse. J Neurosci 18:7779–7799.

Bignami A, Eng LF, Dahl D, Uyeda CT (1972) Localization of the glial fibrillary acidic protein in astrocytes by immunofluorescence. Brain Res 43:429–435.

Brose N (2008) For better or for worse: complexins regulate SNARE function and vesicle fusion. Traffic 9:1403–1413.

Burkhalter A (2008) Many specialists for suppressing cortical excitation. Front Neurosci 2:155–167.

Cadwell CR, Palasantza A, Jiang X, Berens P, Deng Q, Yilmaz M, Reimer J, Shen S, Bethge M, Tolias KF, Sandberg R, Tolias AS (2016) Electrophysiological, transcriptomic and morphologic profiling of single neurons using Patch-seq. Nat Biotechnol 34:199–203.

Cajal SR (2002) Texture of the nervous system of man and the vertebrates, Vol III (Pasik P, Pasik T, eds). New York: Springer.

Chan CH, Godinho LN, Thomaidou D, Tan SS, Gulisano M, Parnavelas JG (2001) *Emx1* is a marker for pyramidal neurons of the cerebral cortex. Cereb Cortex 11:1191–1198.

DeFelipe J, López-Cruz PL, Benavides-Piccione R, Bielza C, Larrañaga P, Anderson S, Burkhalter A, Cauli B, Fairén A, Feldmeyer D, Fishell G, Fitzpatrick D, Freund TF, González-Burgos G, Hestrin S, Hill S, Hof PR, Huang J, Jones EG, Kawaguchi Y, et al. (2013) New insights into the classification and nomenclature of cortical GABAergic interneurons. Nat Rev Neurosci 14:202–216.

Delorme R, Ey E, Toro R, Leboyer M, Gillberg C, Bourgeron T (2013) Progress toward treatments for synaptic defects in autism. Nat Med 19:685–694.

Fishell G, Heintz N (2013) The neuron identity problem: form meets function. Neuron 80:602–612.

Fremeau RT Jr, Troyer MD, Pahner I, Nygaard GO, Tran CH, Reimer RJ, Bellocchio EE, Fortin D, Storm-Mathisen J, Edwards RH (2001) The expression of vesicular glutamate transporters defines two classes of excitatory synapse. Neuron 31:247–260.

Jaitin DA, Kenigsberg E, Keren-Shaul H, Elefant N, Paul F, Zaretsky I, Mildner A, Cohen N, Jung S, Tanay A, Amit I (2014) Massively parallel single-cell RNA-seq for marker-free decomposition of tissues into cell types. Science 343:776–779.

Jiang X, Wang G, Lee AJ, Stornetta RL, Zhu JJ (2013) The organization of two new cortical interneuronal circuits. Nat Neurosci 16:210–218.

Jiang X, Shen S, Cadwell CR, Berens P, Sinz F, Ecker AS, Patel S, Tolias AS (2015) Principles of connectivity among morphologically defined cell types in adult neocortex. Science 350:aac9462.

Kharchenko PV, Silberstein L, Scadden DT (2014) Bayesian approach to single-cell differential expression analysis. Nat Methods 11:740–742.

Lin L, Sun W, Throesch B, Kung F, Decoster JT, Berner CJ, Cheney RE, Rudy B, Hoffman DA (2013) *DPP6* regulation of dendritic morphogenesis impacts hippocampal synaptic development. Nat Commun 4:2270.

Ma J, Yao XH, Fu Y, Yu YC (2014) Development of layer 1 neurons in the mouse neocortex. Cereb Cortex 24:2604–2618.

Macintyre G, Alford T, Xiong L, Rouleau GA, Tibbo PG, Cox DW (2010) Association of *NPAS3* exonic variation with schizophrenia. Schizophr Res 120:143–149.

Macosko EZ, Basu A, Satija R, Nemesh J, Shekhar K, Goldman M, Tirosh I, Bialas AR, Kamitaki N, Martersteck EM, Trombetta JJ, Weitz DA, Sanes JR, Shalek AK, Regev A, McCarroll SA (2015) Highly parallel genome-wide expression profiling of individual cells using nanoliter droplets. Cell 161:1202–1214.

Marshak DR (1990) S100 beta as a neurotrophic factor. Prog Brain Res 86:169–181.

Miyoshi G, Hjerling-Leffler J, Karayannis T, Sousa VH, Butt SJ, Battiste J, Johnson JE, Machold RP, Fishell G (2010) Genetic fate mapping reveals that the caudal ganglionic eminence produces a large and diverse population of superficial cortical interneurons. J Neurosci 30:1582–1594.

Olah S, Fule M, Komlosi G, Varga C, Baldi R, Barzo P, Tamas G (2009) Regulation of cortical microcircuits by unitary GABA-mediated volume transmission. Nature 461:1278–1281.

Picelli S, Bjorklund AK, Faridani OR, Sagasser S, Winberg G, Sandberg R (2013) Smart-seq2 for sensitive full-length transcriptome profiling in single cells. Nat Methods 10:1096–1098.

Petilla Interneuron Nomenclature Group (PING), Ascoli GA, Alonso-Nanclares L, Anderson SA, Barrionuevo G, Benavides-Piccione R, Burkhalter A, Buzsáki G, Cauli B, Defelipe J, Fairén A, Feldmeyer D, Fishell G, Fregnac Y, Freund TF, Gardner D, Gardner EP, Goldberg JH, Helmstaedter M, Hestrin S, et al. (2008) Petilla terminology: nomenclature of features of GABAergic interneurons of the cerebral cortex. Nat Rev Neurosci 9:557–568.

Reimer J, Froudarakis E, Cadwell CR, Yatsenko D, Denfield GH, Tolias AS (2014) Pupil fluctuations track fast switching of cortical states during quiet wakefulness. Neuron 84:355–362.

Sandberg R (2014) Entering the era of single-cell transcriptomics in biology and medicine. Nat Methods 11:22–24.

Siegert S, Cabuy E, Scherf BG, Kohler H, Panda S, Le YZ, Fehling HJ, Gaidatzis D, Stadler MB, Roska B (2012) Transcriptional code and disease map for adult retinal cell types. Nat Neurosci 15:487–495, S481–S482.

Spooren W, Lindemann L, Ghosh A, Santarelli L (2012) Synapse dysfunction in autism: a molecular medicine approach to drug discovery in neurodevelopmental disorders. Trends Pharmacol Sci 33:669–684.

Stanco A, Pla R, Vogt D, Chen Y, Mandal S, Walker J, Hunt RF, Lindtner S, Erdman CA, Pieper AA, Hamilton SP, Xu D, Baraban SC, Rubenstein JL (2014) NPAS1 represses the generation of specific subtypes of cortical interneurons. Neuron 84:940–953.

Stuhmer T, Anderson SA, Ekker M, Rubenstein JL (2002) Ectopic expression of the Dlx genes induces glutamic acid decarboxylase and Dlx expression. Development 129:245–252.

Tang F, Barbacioru C, Wang Y, Nordman E, Lee C, Xu N, Wang X, Bodeau J, Tuch BB, Siddiqui A, Lao K, Surani MA (2009) mRNA-seq whole-transcriptome analysis of a single cell. Nat Methods 6:377–382.

Tasic B, Menon V, Nguyen TN, Kim TK, Jarsky T, Yao Z, Levi B, Gray LT, Sorensen SA, Dolbeare T, Bertagnolli D, Goldy J, Shapovalova N, Parry S, Lee C, Smith K, Bernard A, Madisen L, Sunkin SM, Hawrylycz M, et al. (2016) Adult mouse cortical cell taxonomy revealed by single cell transcriptomics. Nat Neurosci 19:335–346.

Treutlein B, Brownfield DG, Wu AR, Neff NF, Mantalas GL, Espinoza FH, Desai TJ, Krasnow MA, Quake SR (2014) Reconstructing lineage hierarchies of the distal lung epithelium using single-cell RNA-seq. Nature 509:371–375.

Zeisel A, Munoz-Manchado AB, Codeluppi S, Lonnerberg P, La Manno G, Jureus A, Marques S, Munguba H, He L, Betsholtz C, Rolny C, Castelo-Branco G, Hjerling-Leffler J, Linnarsson S (2015) Brain structure. Cell types in the mouse cortex and hippocampus revealed by single-cell RNA-seq. Science 347:1138–1142.